

# Cross-seeding effects of amyloid $\beta$ -protein and $\alpha$ -synuclein

メタデータ	言語: English 出版者: 公開日: 2017-10-03 キーワード (Ja): キーワード (En): 作成者: Ono, Kenjiro, Takahashi, Ryoichi, Ikeda, Tokuhei, Yamada, Masahito メールアドレス: 所属:
URL	<a href="http://hdl.handle.net/2297/34736">http://hdl.handle.net/2297/34736</a>

## Short Communication

### Cross-seeding effects of amyloid $\beta$ -protein and $\alpha$ -synuclein

Kenjiro Ono,<sup>1</sup> Ryoichi Takahashi,<sup>1</sup> Tokuhei Ikeda, and Masahito Yamada

*\* Department of Neurology and Neurobiology and Aging, Kanazawa University Graduate School of Medical Science, Kanazawa, Japan*

Address correspondence and reprint requests to Dr. M. Yamada at Department of Neurology & Neurobiology of Aging, Kanazawa University Graduate School of Medical Science, Kanazawa 920-8640, Japan. E-mail: [m-yamada@med.kanazawa-u.ac.jp](mailto:m-yamada@med.kanazawa-u.ac.jp)

<sup>1</sup> These authors have contributed equally to this study.

*Abbreviations used:* A $\beta$ , amyloid  $\beta$ -protein; AD, Alzheimer's disease; APP, amyloid precursor protein; APS, ammonium persulfate;  $\alpha$ S,  $\alpha$ -synuclein; DLB, dementia with Lewy bodies; EM, electron microscopy; fA $\beta$ , A $\beta$  fibrils; f $\alpha$ S,  $\alpha$ S fibrils; LBD, Lewy body diseases; LBs, Lewy bodies; NAC, non-amyloid component; oligo, cross-linked oligomers; PD, Parkinson disease; PICUP, photo-induced cross-linking of unmodified proteins; Ru(bpy), tris(2,2'-bipyridyl)dichlororuthenium(II) hexahydrate; SDS-PAGE, sodium dodecyl sulfate-polyacrylamide gel electrophoresis; ThS, Thioflavin S; ThT, Thioflavin T.

Amyloid  $\beta$ -protein ( $A\beta$ ) and  $\alpha$ -synuclein ( $\alpha S$ ) are the primary components of amyloid plaques and Lewy bodies (LBs), respectively. Previous *in vitro* and *in vivo* studies have suggested that interactions between  $A\beta$  and  $\alpha S$  are involved in the pathogenesis of Alzheimer's disease (AD) and LB diseases (LBD). However, the seeding effects of their aggregates on their aggregation pathways are not completely clear. To investigate the cross-seeding effects of  $A\beta$  and  $\alpha S$ , we examined how sonicated fibrils or cross-linked oligomers of  $A\beta_{40}$ ,  $A\beta_{42}$ , and  $\alpha S$  affected their aggregation pathways using thioflavin T(S) assay and electron microscopy. Fibrils and oligomers of  $A\beta_{40}$ ,  $A\beta_{42}$ , and  $\alpha S$  acted as seeds, and affected the aggregation pathways within and among species. The seeding effects of  $\alpha S$  fibrils were higher than those of  $A\beta_{40}$  and  $A\beta_{42}$  fibrils in the  $A\beta_{40}$  and  $A\beta_{42}$  aggregation pathways, respectively. We showed that  $A\beta$  and  $\alpha S$  acted as seeds and affected each other's aggregation pathways *in vitro*, which may contribute to our understanding of the molecular mechanisms of interactions between AD and LBD pathologies.

*Key words:*  $\alpha$ -synuclein, aggregation, Alzheimer's disease, amyloid  $\beta$ -protein, Lewy body diseases, seed

*Running head:* Cross-seeding effects of  $A\beta$  and  $\alpha S$

Amyloid  $\beta$ -protein (A $\beta$ ) and  $\alpha$ -synuclein ( $\alpha$ S) are the primary components of amyloid plaques and Lewy bodies (LBs), respectively. Aggregations of A $\beta$  and  $\alpha$ S are considered to be a critical step during neurodegeneration associated with Alzheimer's disease (AD) and Lewy body diseases (LBD), respectively. AD is characterized by the accumulation of A $\beta$  plaques and neurofibrillary tangles. Interestingly, up to 50% of AD cases exhibit significant LB pathology in addition to plaques and tangles (Hamilton 2000). Likewise, patients with dementia with LBs (DLB) frequently exhibit AD pathology, particularly senile plaques (Armstrong *et al.* 1997).

Recent studies suggest that accumulations of oligomers might be the neurotoxic species, rather than fibrils. The progressive accumulation of A $\beta$  oligomers has been identified as a central toxic event during AD that leads to synaptic dysfunction (Ono & Yamada 2011), whereas the formation of  $\alpha$ S oligomers that disrupt membrane and mitochondrial activity has been linked to LBD (Kim *et al.* 2009).

It was previously shown that A $\beta$  enhances  $\alpha$ S accumulation and neuronal deficits using transgenic mice with neuronal expression of A $\beta$  and  $\alpha$ S (Masliah *et al.* 2001). NMR study showed that A $\beta$  and  $\alpha$ S might interact directly at a few sites (Mandal *et al.* 2006). A recent *in vitro* study reported that A $\beta$  and  $\alpha$ S might interact directly to form hybrid pore-like oligomers that contribute to neurodegeneration (Tsigelny *et al.* 2008). These studies suggest that interactions between A $\beta$  and  $\alpha$ S are involved in the pathogenesis of AD and LBD, but the seeding effects of their aggregates on aggregation pathways have not been elucidated. Thus, we determined whether fibrils or cross-linked oligomers of A $\beta$ 40, A $\beta$ 42, and  $\alpha$ S have cross-seeding effects on each other's aggregation pathways *in vitro*.

## **Materials and methods**

### **Preparation of peptides**

A $\beta$  and  $\alpha$ S solutions were prepared as described previously (Ono *et al.* 2003, Ono & Yamada 2006). A $\beta$ 40 and A $\beta$ 42 were purchased from Peptide Institute Inc. (Osaka, Japan). A $\beta$  lyophilizates were dissolved at 25  $\mu$ M in 10% (v/v) 60 mM NaOH and 90% (v/v) 10 mM

phosphate buffer, pH 7.4.  $\alpha$ S was purchased from Recombinant Peptide Technologies (LLC, GA).  $\alpha$ S was dissolved at 25  $\mu$ M in 20 mM Tris buffer, pH 7.4. After sonication for 1 min using a bath sonicator, A $\beta$  and  $\alpha$ S solutions were centrifuged for 10 min at  $16,000 \times g$ .

### **Preparation of fibrils**

The resulting supernatant was incubated at 37°C for 2 (A $\beta$ 42) or 10 (A $\beta$ 40,  $\alpha$ S) days. Fibril preparations were stored as lyophilizates and reconstituted at 25  $\mu$ M in 10 mM phosphate buffer or 20 mM Tris buffer. After sonication on ice with 30 intermittent pulses using an ultrasonic disruptor, the sonicated A $\beta$ 40 fibrils (fA $\beta$ 40), A $\beta$ 42 fibrils (fA $\beta$ 42), and  $\alpha$ S fibrils (f $\alpha$ S) were used for the **seeding** assays.

### **Thioflavin T (ThT) and thioflavin S (ThS) binding**

The reaction mixture contained 5  $\mu$ M ThT (Wako Chemical Industries Ltd, Osaka, Japan) or ThS (MP Biomedicals, Irvine, CA) and 50 mM of glycine-NaOH buffer, pH 8.5. After vortexing briefly, fluorescence was determined three times at intervals of 10 s using a Hitachi F-2500 fluorometer. Excitation and emission wavelengths of 445 and 490 nm were used for the A $\beta$ 40 and A $\beta$ 42 assays, respectively. Excitation and emission wavelengths of 440 and 521 nm were used for  $\alpha$ S assay, respectively. Fluorescence was determined by averaging three readings and subtracting the ThT or ThS blank readings.

### **Photo-induced cross-linking of unmodified proteins (PICUP) and sodium dodecyl sulfate-polyacrylamide gel electrophoresis (SDS-PAGE)**

Cross-linking of A $\beta$ 40, A $\beta$ 42, or  $\alpha$ S was photo-induced, essentially as previously described (Ono *et al.* 2008, Ono *et al.* 2011b). To 18  $\mu$ l of 25  $\mu$ M protein solution, we added 1  $\mu$ l of 2-4 mM tris(2,2'-bipyridyl)dichlororuthenium(II) (Ru(bpy)) and 1  $\mu$ l of 40-80 mM ammonium persulfate. The mixtures were irradiated for 1 s with visible light and the reaction was quenched with 1  $\mu$ l of 1 M dithiothreitol (DTT) (Invitrogen) in ultrapure water. The frequency distribution of monomers and oligomers was determined using SDS-PAGE and silver staining, as described previously (Ono *et al.* 2008).

### **Size-exclusion chromatography (SEC)**

PICUP reagents were removed from cross-linked samples by SEC as described previously (Ono *et al.* 2010). A $\beta$  and  $\alpha$ S peptides were eluted in the void volume, whereas Ru(bpy), APS, and DTT entered the column matrix separately from A $\beta$  or  $\alpha$ S. Fractions were lyophilized immediately after collection. The lyophilizates were reconstituted at 25  $\mu$ M.

### **Seeding activity of fibril and cross-linked oligomers of A $\beta$ 40, A $\beta$ 42, and $\alpha$ S**

Fibrils or cross-linked oligomers (oligo) of A $\beta$ 40, A $\beta$ 42, or  $\alpha$ S were prepared at a concentration of 25 or 5  $\mu$ M in 10mM phosphate buffer or 20 mM Tris buffer, pH 7.4. For the seeding assays, sonicated fibrils (Fig. 1) or cross-linked peptides (Fig. 1) were added as seeds to un-cross-linked peptides at a ratio of 10% (v/v). The mixtures were incubated at 37°C for 0–7 days.

### **Electron microscopy (EM)**

A 10- $\mu$ l aliquot of each sample was spotted onto a glow-discharged, carbon-coated formvar grid (Okenshoji Co. Ltd, Tokyo, Japan) and incubated for 20 min. The droplet was displaced with an equal volume of 2.5% (v/v) glutaraldehyde in water and incubated for an additional 5 min. Finally, the peptide was stained with 8  $\mu$ l of 1% (v/v) uranyl acetate in water (Wako Chemical Industries Ltd). This solution was wicked off and the grid was air-dried. Samples were examined using a JEM-1210 transmission electron microscope.

### **Statistical analysis**

One-way factorial ANOVA followed by Bonferroni *post hoc* comparisons were used to determine statistical significance among data sets. These tests were implemented within GraphPad Prism software (version 4.0a, GraphPad Software, Inc., San Diego, CA). Significance was defined as  $p < 0.05$ .

## **Results and discussion**

We used a well-characterized assay of fibril formation, thioflavin dye binding (LeVine 1999), to determine the effects of fibrils or cross-linked oligomers on peptide assembly. In order to compare their seeding effects precisely, we arranged A $\beta$ 40, A $\beta$ 42, and  $\alpha$ S solutions with the same concentration (25  $\mu$ M), at which oligo A $\beta$ 40 and oligo A $\beta$ 42 functioned as seeds during A $\beta$

assembly (Ono *et al.* 2009, Ono *et al.* 2010). As shown in Fig. 2A, the ThT fluorescence followed a sigmoidal curve when fresh A $\beta$ 40 was incubated at 37°C, which was characterized by a ~1 day lag time, a ~5 day period of increasing ThT binding, and a plateau after ~6 days. This curve is consistent with a nucleation-dependent polymerization model (Jarrett & Lansbury 1993, Ono *et al.* 2003). When fresh A $\beta$ 40 was incubated with fA $\beta$ 40 at 37°C, the fluorescence increased hyperbolically without a lag phase, and a plateau occurred after ~4 h (Fig. 2A). This curve is consistent with a first-order kinetic model (Ono *et al.* 2003). Similar effects were observed after the addition of fA $\beta$ 42 or f $\alpha$ S. The growth rates of fA $\beta$ 42 and f $\alpha$ S were 27.9 and 64.8 FU/h, respectively, while the rate of fA $\beta$ 42 was significantly lower ( $p < 0.01$ ) than those of fA $\beta$ 40 (68.6 FU/h) and f $\alpha$ S. The plateau occurred after ~2 h with f $\alpha$ S, which was earlier than that with fA $\beta$ 40 (~4 h). Fluorescence also increased hyperbolically without a lag phase when fresh A $\beta$ 40 was incubated with oligo A $\beta$ 40 at 37°C and a plateau occurred after ~48 h (Fig. 2A). Similar effects were observed after the addition of oligo A $\beta$ 42 or oligo  $\alpha$ S, though their growth rates (oligo A $\beta$ 42, 8.1 FU/h; oligo  $\alpha$ S, 6.4 FU/h) were significantly lower ( $p < 0.05$ ) than that produced by oligo A $\beta$ 40 (9.6 FU/h). Overall, the seeding effects during A $\beta$ 40 assembly were in the order of f $\alpha$ S  $\geq$  fA $\beta$ 40 > fA $\beta$ 42 >> oligo A $\beta$ 40 > oligo A $\beta$ 42 > oligo  $\alpha$ S. As shown in Fig. 2B, fA $\beta$ 40 produced with a fresh A $\beta$ 40 solution assumed a nonbranched, helical filament structure of ~7 nm with a helical periodicity of approximately 220 nm, as described previously (Ono *et al.* 2003, Ono *et al.* 2008). A typical fibrillar structure was also observed when A $\beta$ 40 was incubated with fA $\beta$ 40, fA $\beta$ 42, f $\alpha$ S, oligo A $\beta$ 40, oligo A $\beta$ 42, or oligo  $\alpha$ S (Figs. 2C-H). At lower concentration (5  $\mu$ M), f $\alpha$ S acted as seeds (growth rate, 9.6 FU/h) although oligo  $\alpha$ S did not.

Similar results were obtained for A $\beta$ 42 assembly. As shown in Fig. 3A, the ThT fluorescence produced a sigmoidal curve when fresh A $\beta$ 42 was incubated at 37°C, which was characterized by a ~2-h lag time, a ~10-h period of increasing ThT binding, and a plateau after ~12 h. The fluorescence increased hyperbolically without a lag phase when fresh A $\beta$ 42 was incubated with fA $\beta$ 42 at 37°C and a binding plateau occurred after ~2 h (Fig. 3A). A similar effect was observed after the addition of fA $\beta$ 40 or f $\alpha$ S. The growth rates of fA $\beta$ 42, fA $\beta$ 40, and f $\alpha$ S were 48.9, 41.5, and 54.2 FU/h, respectively, while the rates of fA $\beta$ 42 and f $\alpha$ S were significantly higher ( $p < 0.01$ ) than that of fA $\beta$ 40. The fluorescence also increased hyperbolically without a lag phase when fresh A $\beta$ 42 was incubated with oligo A $\beta$ 42 at 37°C and a plateau occurred after ~4 h (Fig. 3A). Similar effects were observed after the addition of oligo A $\beta$ 40 or oligo  $\alpha$ S, although their

growth rates (oligo A $\beta$ 40, 24.7 FU/h; oligo  $\alpha$ S, 21.5 FU/h) were lower than that of oligo A $\beta$ 42 (38.0 FU/h) ( $p < 0.01$ ). Overall, the seeding effects during A $\beta$ 42 assembly were in the order of f $\alpha$ S  $\geq$  fA $\beta$ 42  $>$  fA $\beta$ 40  $>>$  oligo A $\beta$ 42  $\geq$  oligo A $\beta$ 40  $>$  oligo  $\alpha$ S. As shown in Fig. 3B, fresh A $\beta$ 42 solution formed nonbranched filaments with a width of  $\sim$ 8 nm and varying degrees of helicity, as described previously (Ono *et al.* 2003, Ono *et al.* 2008). We also observed thicker, straight, non-branched filaments with a width of  $\sim$ 12 nm. Typical fibrillar structures were also observed when A $\beta$ 42 was incubated with fA $\beta$ 42, fA $\beta$ 40, f $\alpha$ S, oligo A $\beta$ 42, oligo A $\beta$ 40, or oligo  $\alpha$ S (Figs. 3C-H). At lower concentration (5  $\mu$ M), f $\alpha$ S acted as seeds (growth rate, 15.2 FU/h) although oligo  $\alpha$ S did not.

We monitored the kinetics of  $\alpha$ S assembly using ThS assay to determine whether  $\alpha$ S assembly was affected by homogeneous or heterogeneous fibrils or oligomers.  $\alpha$ S produced a sigmoidal curve in the absence of any fibrils or oligomers, which was characterized by a lag time of 12 h, a period of increasing ThS binding for 4.5 days, and a plateau after 5 days (Fig. 4A)—results consistent with the nucleation-dependent polymerization model (Wood *et al.* 1999). The binding curves increased hyperbolically without a lag phase when  $\alpha$ S was incubated with f $\alpha$ S and a plateau occurred after  $\sim$ 6 h (Fig. 4A). A similar effect was observed after the addition of fA $\beta$ 40 or fA $\beta$ 42, though their growth rates were different. The growth rates of f $\alpha$ S, fA $\beta$ 40, and fA $\beta$ 42 were 25.0, 11.3, and 18.9 FU/h, respectively, while the rate of f $\alpha$ S was significantly higher ( $p < 0.05$ ) than that of fA $\beta$ 40 or fA $\beta$ 42. The fluorescence also increased hyperbolically without a lag phase when fresh  $\alpha$ S was incubated with oligo  $\alpha$ S at 37°C and a plateau occurred after  $\sim$ 3 days (Fig. 4A). Similar effects were observed after the addition of oligo A $\beta$ 40 or oligo A $\beta$ 42, though their growth rates (oligo A $\beta$ 40, 3.7 FU/h; oligo A $\beta$ 42, 4.7 FU/h) were significantly lower than oligo  $\alpha$ S (6.1 FU/h) ( $p < 0.01$ ). Overall, the seeding effects during  $\alpha$ S assembly were in the order of f $\alpha$ S  $>$  fA $\beta$ 42  $>$  fA $\beta$ 40  $>>$  oligo  $\alpha$ S  $>$  oligo A $\beta$ 42  $>$  oligo A $\beta$ 40. We observed nonbranched, helical filaments with diameters of 10 nm after the incubation of fresh  $\alpha$ S (Fig. 4B). Typical fibrillar structures were also observed when  $\alpha$ S was incubated with f $\alpha$ S, fA $\beta$ 40, fA $\beta$ 42, oligo  $\alpha$ S, oligo A $\beta$ 40, or oligo A $\beta$ 42 (Figs. 4C-H).

Previously, we reported that sonicated fibrils and cross-linked oligomers functioned as seeds during A $\beta$  and  $\alpha$ S assembly (Ono *et al.* 2003, Ono *et al.* 2009, Ono *et al.* 2010, Ono *et al.* 2011a). Our used PICUP-stabilized oligomers have significant biochemical properties such as increased neurotoxic activity and  $\beta$ -sheet ratios of secondary structures with higher oligomer



order (Ono *et al.* 2009, Ono *et al.* 2010, Ono *et al.* 2011a). The current study showed that fibrils and cross-linked oligomers of A $\beta$ 40, fA $\beta$ 42, and f $\alpha$ S had seeding effects on the aggregation pathways of different species and the same species. The seeding effects of oligomers were lower than those of fibrils. Interestingly, the seeding effect of f $\alpha$ S was higher than that of fA $\beta$ 40 on A $\beta$ 40 aggregation. Similarly, the seeding effect of f $\alpha$ S was higher than that of fA $\beta$ 42 on A $\beta$ 42 aggregation. The seeding effects of fA $\beta$ 42 and fA $\beta$ 40 on the  $\alpha$ S aggregation pathway were lower than that of f $\alpha$ S.

The molecular mechanisms underlying the interactions between A $\beta$ 40, A $\beta$ 42, and  $\alpha$ S need to be considered. The hydrophobic core of A $\beta$ , i.e., residues 17-21, is known to play an important role in the formation and stabilization of amyloid fibrils (Wood *et al.* 1995). Similarly, a central hydrophobic non-amyloid component (NAC) region (residues 61-95) is also essential for  $\alpha$ S aggregation (Lucking & Brice 2000). NAC is known to promote A $\beta$  aggregation by binding 81-95 residues of NAC via 25-35 A $\beta$  residues (Yoshimoto *et al.* 1995). A previous NMR study also showed that  $\alpha$ S might interact directly with A $\beta$  at a few sites, i.e., G67, G73, and V74, belonging to NAC (Mandal *et al.* 2006). It was reported that A $\beta$  facilitated the formation of more stable  $\alpha$ S oligomers via direct interaction with NAC *in vitro* (Tsigelny, *et al.* 2008). In our study, it was interesting that the fibrillar form of  $\alpha$ S accelerated the A $\beta$ 40 and A $\beta$ 42 aggregations more rapidly than fA $\beta$ 40 and fA $\beta$ 42. Previously, Naiki's group analyzed the interaction effects of A $\beta$ 40 and A $\beta$ 42 on the kinetics of *in vitro* fA $\beta$ s formation using ThT assay (Hasegawa *et al.* 1999). The aggregation of fresh A $\beta$ 40 was accelerated by the addition of fA $\beta$ 42, though the effect was lower compared with the addition of fA $\beta$ 40 to A $\beta$ 40 (Hasegawa *et al.* 1999). The fluorescence increased hyperbolically without a lag phase when A $\beta$ 42 was incubated with fA $\beta$ 40 and it proceeded to equilibrium more rapidly than without fA $\beta$ 40 (Hasegawa *et al.* 1999). It was also suggested that the hydrophobic core may contribute to the association between A $\beta$ 40 and A $\beta$ 42 (Hasegawa *et al.* 1999). The hydrophobic cores of A $\beta$ 40, A $\beta$ 42, and  $\alpha$ S may also contribute to their monomer-fibril association with each other. In particular, the hydrophobic core of  $\alpha$ S might have stronger promoting effects than those of A $\beta$ 40 and A $\beta$ 42.

Several *in vivo* studies have focused on understanding the direct interaction of A $\beta$  and  $\alpha$ S. Masliah *et al.* (2001) showed that A $\beta$  promotes the *in vivo* aggregation of  $\alpha$ S while it exacerbates learning deficits with amyloid precursor protein (APP)/ $\alpha$ S double transgenic mice.  $\alpha$ S has also been shown to accumulate in the brains of Tg2576 mice (Yang *et al.* 2000) and APP/presenilin-1

double transgenic mice, which produce large amounts of A $\beta$  (Kurata *et al.* 2007). More importantly, several studies using human brains have shown that A $\beta$  contributes to the levels and status of  $\alpha$ S aggregation and LB formation (Lippa *et al.* 2005, Pletnikova *et al.* 2005). Lippa *et al.* (2005) compared the amygdala of subjects with pathological aging and AD. The A $\beta$ 40 plaque level was higher in cases with secondary  $\alpha$ S aggregates. The A $\beta$ 42 plaque level was not associated with  $\alpha$ S aggregation. Pletnikova *et al.* (2005) examined autopsied brains from 21 cases of LBD. In brains without A $\beta$  deposits, there was little or no LB in the cerebral cortex. In contrast, they observed significant increases in LB in the cerebral cortex and  $\alpha$ S immunoreactive lesions in the cingulate cortex of brains with A $\beta$  deposits (Pletnikova *et al.* 2005). Immunoblots of  $\alpha$ S from the cingulate cortex of brains with A $\beta$  deposits indicated significantly higher levels of insoluble  $\alpha$ S compared with brains without A $\beta$  deposits (Pletnikova *et al.* 2005). Overall, these studies of transgenic mice and human brains support a hypothesis that A $\beta$  and  $\alpha$ S interact *in vivo* and that these interactions are of significance for the pathogenesis of the disease. The mechanisms of extracellular A $\beta$  and intracellular  $\alpha$ S interaction are unclear, but there have been some significant reports. Agnati *et al.* (2010) suggested that A $\beta$  and  $\alpha$ S cannot diffuse via the extracellular space but that they can move from cell to cell via tunneling nanotubes, which may propagate mitochondrial damage and cell degeneration. This was supported by the presence of A $\beta$  and  $\alpha$ S within intracellular nanotubes. Indeed, A $\beta$  monomers and oligomers have been detected intracellularly in the brains of AD patients (Walsh *et al.* 2000, Steiner *et al.* 2008), while  $\alpha$ S monomers and oligomers were detected extracellularly in biological fluids, such as the blood plasma and cerebrospinal fluid of LBD patients (El-Agnaf *et al.* 2003, Tokuda *et al.* 2010). Thus, it is possible that the oligomers and monomers of A $\beta$  and  $\alpha$ S might promote the aggregation of each other both intracellularly and extracellularly.

The seeded proliferation of misfolded proteins that occurs during prion disease may explain the pathogenesis of AD and LBD. The pathological similarities between prion disease and AD have long engendered the speculation that AD might be inducible in a prion-like manner (Gajdusek 1994). The Jucker group reported that the seeding of A $\beta$  deposition was ineffective in nontransgenic mice, while the phenotype of induced A $\beta$  deposits in transgenic mice mirrored that of deposits in the extract, thereby implicating an A $\beta$ -templating mechanism (Meyer-Luehmann *et al.* 2006, Eisele *et al.* 2009). It was also shown that soluble extracts of A $\beta$  deposits could act as amyloid-inducing seeds (Langer *et al.* 2011). Increasing evidence implicates the templated

corruption of disease-specific proteins in other neurodegenerative diseases such as LBD. A seeding-like process in  $\alpha$ S lesions was bolstered by the observation that fetal dopaminergic neural transplants in the striatum of PD patients can eventually lead to the presence of  $\alpha$ S-positive LBs in some cells, suggesting that  $\alpha$ S seeds propagate from the host to the graft (Li *et al.* 2008, Kordower *et al.* 2008). *In vitro* cross-seeding effects have never been reported before, but our *in vitro* study indicated that aggregates of A $\beta$  and  $\alpha$ S acted as seeds and promoted the aggregation of each other.

In conclusion, the fibrils and oligomers of A $\beta$ 40, A $\beta$ 42, and  $\alpha$ S functioned as seeds and promoted each other's aggregation pathways, though the oligomers were less efficient than fibrils. The cross-seeding effects observed in this study may provide new insights into the molecular mechanisms that underlie the interactions between AD and LBD pathogenesis.

## Acknowledgements

The authors acknowledge the support of Grant-in-Aid for Challenging Exploratory Research (22659170) (M.Y.), and Knowledge Cluster Initiative [High-Tech Sensing and Knowledge Handling Technology (Brain Technology)] (M.Y.) from the Japanese Ministry of Education, Culture, Sports, Science and Technology, Japan, a grant to the Amyloidosis Research Committee from the Ministry of Health, Labor, and Welfare, Japan (M.Y.), Grants-in-Aid for Young Scientists (B) (K.O.), Alumni Association of the Department of Medicine at Showa University (K.O.), Kanae Foundation for the Promotion of Medical Science (K.O.), and Nagao Memorial fund (K.O.). The authors have no conflict of interest to declare.

## References

- Agnati, L. F., Guidolin, D., Baluska, F., Leo, G., Barlow, P. W., Carone, C. and Genedani, S. (2010) A new hypothesis of pathogenesis based on the divorce between mitochondria and their host cells: possible relevance for Alzheimer's disease. *Curr Alzheimer Res*, **7**, 307-322.
- Armstrong, R. A., Cairns, N. J. and Lantos, P. L. (1997)  $\beta$ -Amyloid ( $A\beta$ ) deposition in the medial temporal lobe of patients with dementia with Lewy bodies. *Neurosci Lett*, **227**, 193-196.
- Eisele, Y. S., Bolmont, T., Heikenwalder, M. et al. (2009) Induction of cerebral  $\beta$ -amyloidosis: intracerebral versus systemic A $\beta$  inoculation. *Proc Natl Acad Sci U S A*, **106**, 12926-12931.
- El-Agnaf, O. M., Salem, S. A., Paleologou, K. E. et al. (2003)  $\alpha$ -synuclein implicated in Parkinson's disease is present in extracellular biological fluids, including human plasma. *FASEB J*, **17**, 1945-1947.
- Gajdusek, D. C. (1994) Spontaneous generation of infectious nucleating amyloids in the transmissible and nontransmissible cerebral amyloidoses. *Mol Neurobiol*, **8**, 1-13.
- Hamilton, R. L. (2000) Lewy bodies in Alzheimer's disease: a neuropathological review of 145 cases using  $\alpha$ -synuclein immunohistochemistry. *Brain Pathol*, **10**, 378-384.
- Hasegawa, K., Yamaguchi, I., Omata, S., Gejyo, F. and Naiki, H. (1999) Interaction between  $A\beta(1-42)$  and  $A\beta(1-40)$  in Alzheimer's  $\beta$ -amyloid fibril formation in vitro. *Biochemistry*, **38**, 15514-15521.
- Jarrett, J. T. and Lansbury, P. T., Jr. (1993) Seeding "one-dimensional crystallization" of amyloid: a pathogenic mechanism in Alzheimer's disease and scrapie? *Cell*, **73**, 1055-1058.
- Kim, H. Y., Cho, M. K., Kumar, A. et al. (2009) Structural properties of pore-forming oligomers of  $\alpha$ -synuclein. *J Am Chem Soc*, **131**, 17482-17489.
- Kordower, J. H., Chu, Y., Hauser, R. A., Freeman, T. B. and Olanow, C. W. (2008) Lewy body-like pathology in long-term embryonic nigral transplants in Parkinson's disease. *Nat Med*, **14**, 504-506.
- Kurata, T., Kawarabayashi, T., Murakami, T. et al. (2007) Enhanced accumulation of phosphorylated  $\alpha$ -synuclein in double transgenic mice expressing mutant  $\beta$ -amyloid

- precursor protein and presenilin-1. *J Neurosci Res*, **85**, 2246-2252.
- Langer, F., Eisele, Y. S., Fritschi, S. K., Staufenbiel, M., Walker, L. C. and Jucker, M. (2011) Soluble A $\beta$  seeds are potent inducers of cerebral  $\beta$ -amyloid deposition. *J Neurosci*, **31**, 14488-14495.
- LeVine, H., 3rd (1999) Quantification of  $\beta$ -sheet amyloid fibril structures with thioflavin T. *Methods Enzymol*, **309**, 274-284.
- Li, J. Y., Englund, E., Holton, J. L. et al. (2008) Lewy bodies in grafted neurons in subjects with Parkinson's disease suggest host-to-graft disease propagation. *Nat Med*, **14**, 501-503.
- Lippa, S. M., Lippa, C. F. and Mori, H. (2005)  $\alpha$ -Synuclein aggregation in pathological aging and Alzheimer's disease: the impact of  $\beta$ -amyloid plaque level. *Am J Alzheimers Dis Other Dement*, **20**, 315-318.
- Lucking, C. B. and Brice, A. (2000)  $\alpha$ -synuclein and Parkinson's disease. *Cell Mol Life Sci*, **57**, 1894-1908.
- Mandal, P. K., Pettegrew, J. W., Masliah, E., Hamilton, R. L. and Mandal, R. (2006) Interaction between A $\beta$  peptide and  $\alpha$  synuclein: molecular mechanisms in overlapping pathology of Alzheimer's and Parkinson's in dementia with Lewy body disease. *Neurochem Res*, **31**, 1153-1162.
- Masliah, E., Rockenstein, E., Veinbergs, I., Sagara, Y., Mallory, M., Hashimoto, M. and Mucke, L. (2001)  $\beta$ -amyloid peptides enhance  $\alpha$ -synuclein accumulation and neuronal deficits in a transgenic mouse model linking Alzheimer's disease and Parkinson's disease. *Proc Natl Acad Sci U S A*, **98**, 12245-12250.
- Meyer-Luehmann, M., Coomaraswamy, J., Bolmont, T. et al. (2006) Exogenous induction of cerebral  $\beta$ -amyloidogenesis is governed by agent and host. *Science*, **313**, 1781-1784.
- Ono, K., Condrón, M. M., Ho, L., Wang, J., Zhao, W., Pasinetti, G. M. and Teplow, D. B. (2008) Effects of grape seed-derived polyphenols on amyloid  $\beta$ -protein self-assembly and cytotoxicity. *J Biol Chem*, **283**, 32176-32187.
- Ono, K., Condrón, M. M. and Teplow, D. B. (2009) Structure-neurotoxicity relationships of amyloid  $\beta$ -protein oligomers. *Proc Natl Acad Sci U S A*, **106**, 14745-14750.
- Ono, K., Condrón, M. M. and Teplow, D. B. (2010) Effects of the English (H6R) and Tottori (D7N) familial Alzheimer disease mutations on amyloid  $\beta$ -protein assembly and toxicity. *J Biol Chem*, **285**, 23186-23197.

- Ono, K., Ikeda, T., Takasaki, J. and Yamada, M. (2011a) Familial Parkinson disease mutations influence  $\alpha$ -synuclein assembly. *Neurobiol Dis*, **43**, 715-724.
- Ono, K., Mochizuki, H., Ikeda, T., Nihira, T., Takasaki, J. I., Teplow, D. B. and Yamada, M. (2011b) Effect of melatonin on  $\alpha$ -synuclein self-assembly and cytotoxicity. *Neurobiol Aging*, in press.
- Ono, K. and Yamada, M. (2006) Antioxidant compounds have potent anti-fibrillogenic and fibril-destabilizing effects for  $\alpha$ -synuclein fibrils in vitro. *J Neurochem*, **97**, 105-115.
- Ono, K. and Yamada, M. (2011) Low-n oligomers as therapeutic targets of Alzheimer's disease. *J Neurochem*, **117**, 19-28.
- Ono, K., Yoshiike, Y., Takashima, A., Hasegawa, K., Naiki, H. and Yamada, M. (2003) Potent anti-amyloidogenic and fibril-destabilizing effects of polyphenols in vitro: implications for the prevention and therapeutics of Alzheimer's disease. *J Neurochem*, **87**, 172-181.
- Pletnikova, O., West, N., Lee, M. K., Rudow, G. L., Skolasky, R. L., Dawson, T. M., Marsh, L. and Troncoso, J. C. (2005) A $\beta$  deposition is associated with enhanced cortical  $\alpha$ -synuclein lesions in Lewy body diseases. *Neurobiol Aging*, **26**, 1183-1192.
- Steinerman, J. R., Irizarry, M., Scarmeas, N., Raju, S., Brandt, J., Albert, M., Blacker, D., Hyman, B. and Stern, Y. (2008) Distinct pools of  $\beta$ -amyloid in Alzheimer disease-affected brain: a clinicopathologic study. *Arch Neurol*, **65**, 906-912.
- Tokuda, T., Qureshi, M. M., Ardah, M. T. et al. (2010) Detection of elevated levels of  $\alpha$ -synuclein oligomers in CSF from patients with Parkinson disease. *Neurology*, **75**, 1766-1772.
- Tsigelny, I. F., Crews, L., Desplats, P. et al. (2008) Mechanisms of hybrid oligomer formation in the pathogenesis of combined Alzheimer's and Parkinson's diseases. *PLoS One*, **3**, e3135.
- Walsh, D. M., Tseng, B. P., Rydel, R. E., Podlisny, M. B. and Selkoe, D. J. (2000) The oligomerization of amyloid  $\beta$ -protein begins intracellularly in cells derived from human brain. *Biochemistry*, **39**, 10831-10839.
- Wood, S. J., Wetzel, R., Martin, J. D. and Hurle, M. R. (1995) Prolines and amyloidogenicity in fragments of the Alzheimer's peptide  $\beta$ /A4. *Biochemistry*, **34**, 724-730.
- Wood, S. J., Wypych, J., Steavenson, S., Louis, J. C., Citron, M. and Biere, A. L. (1999)  $\alpha$ -synuclein fibrillogenesis is nucleation-dependent. Implications for the pathogenesis of

Parkinson's disease. *J Biol Chem*, **274**, 19509-19512.

Yang, F., Ueda, K., Chen, P., Ashe, K. H. and Cole, G. M. (2000) Plaque-associated  $\alpha$ -synuclein (NACP) pathology in aged transgenic mice expressing amyloid precursor protein. *Brain Res*, **853**, 381-383.

Yoshimoto, M., Iwai, A., Kang, D., Otero, D. A., Xia, Y. and Saitoh, T. (1995) NACP, the precursor protein of the non-amyloid  $\beta$ /A4 protein ( $A\beta$ ) component of Alzheimer disease amyloid, binds  $A\beta$  and stimulates  $A\beta$  aggregation. *Proc Natl Acad Sci U S A*, **92**, 9141-9145.

## Figure Legends

**Fig. 1. Morphology of sonicated fibrils and oligomers of A $\beta$ 40, A $\beta$ 42, and  $\alpha$ S.** EM was used to determine the morphologies of fA $\beta$ 40 (A), fA $\beta$ 42 (B), f $\alpha$ S (C), oligo A $\beta$ 40 (D), oligo A $\beta$ 42 (E), and oligo  $\alpha$ S (F). Scale bars indicate 100 nm.

**Fig. 2. Cross seeding effects of A $\beta$ 40 with A $\beta$ 42 or  $\alpha$ S.** (A) ThT binding. A 25- $\mu$ M A $\beta$ 40 solution was incubated without ( $\diamond$ ) or with 10% (v/v) fA $\beta$ 40 ( $\circ$ ), fA $\beta$ 42 ( $\Delta$ ), f $\alpha$ S ( $\square$ ), cross-linked oligomers (oligo) of A $\beta$ 40 ( $\bullet$ ), A $\beta$ 42 ( $\blacktriangle$ ), or  $\alpha$ S ( $\square$ ). Binding is expressed as the mean fluorescence (FU)  $\pm$  S.E. (B-H) A $\beta$ 40 assembly morphology. EM was used to determine the morphologies of assemblies of A $\beta$ 40 without (B) or with fA $\beta$ 40 (C), fA $\beta$ 42 (D), f $\alpha$ S (E), oligo A $\beta$ 40 (F), oligo A $\beta$ 42 (G), or oligo  $\alpha$ S (H). Scale bars indicate 100 nm.

**Fig. 3. Cross seeding effects of A $\beta$ 42 with A $\beta$ 40 or  $\alpha$ S.** (A) ThT binding. A 25- $\mu$ M A $\beta$ 42 solution was incubated without ( $\diamond$ ) or with 10% (v/v) fA $\beta$ 42 ( $\Delta$ ), fA $\beta$ 40 ( $\circ$ ), f $\alpha$ S ( $\square$ ), oligo A $\beta$ 42 ( $\blacktriangle$ ), oligo A $\beta$ 40 ( $\bullet$ ), or oligo  $\alpha$ S ( $\square$ ). Binding is expressed as the mean fluorescence (FU)  $\pm$  S.E. (B-H) A $\beta$ 42 assembly morphology. EM was used to determine the morphologies of assemblies of A $\beta$ 42 without (B) or with fA $\beta$ 42 (C), fA $\beta$ 40 (D), f $\alpha$ S (E), oligo A $\beta$ 42 (F), oligo A $\beta$ 40 (G), or oligo  $\alpha$ S (H). Scale bars indicate 100 nm.

**Fig. 4. Cross seeding effects of  $\alpha$ S with A $\beta$ 40 or A $\beta$ 42.** (A) ThS binding. A 25- $\mu$ M  $\alpha$ S solution was incubated without ( $\diamond$ ) or with 10% (v/v) f $\alpha$ S ( $\square$ ), fA $\beta$ 40 ( $\circ$ ), fA $\beta$ 42 ( $\Delta$ ), oligo  $\alpha$ S ( $\square$ ), oligo A $\beta$ 40 ( $\bullet$ ), or oligo A $\beta$ 42 ( $\blacktriangle$ ). Binding is expressed as the mean fluorescence (FU)  $\pm$  S.E. (B-H)  $\alpha$ S assembly morphology. EM was used to determine the morphologies of assemblies of  $\alpha$ S without (B) or with f $\alpha$ S (C), fA $\beta$ 40 (D), fA $\beta$ 42 (E), oligo  $\alpha$ S (F), oligo A $\beta$ 40 (G), or oligo A $\beta$ 42 (H). Scale bars indicate 100 nm.



Fig. 1.

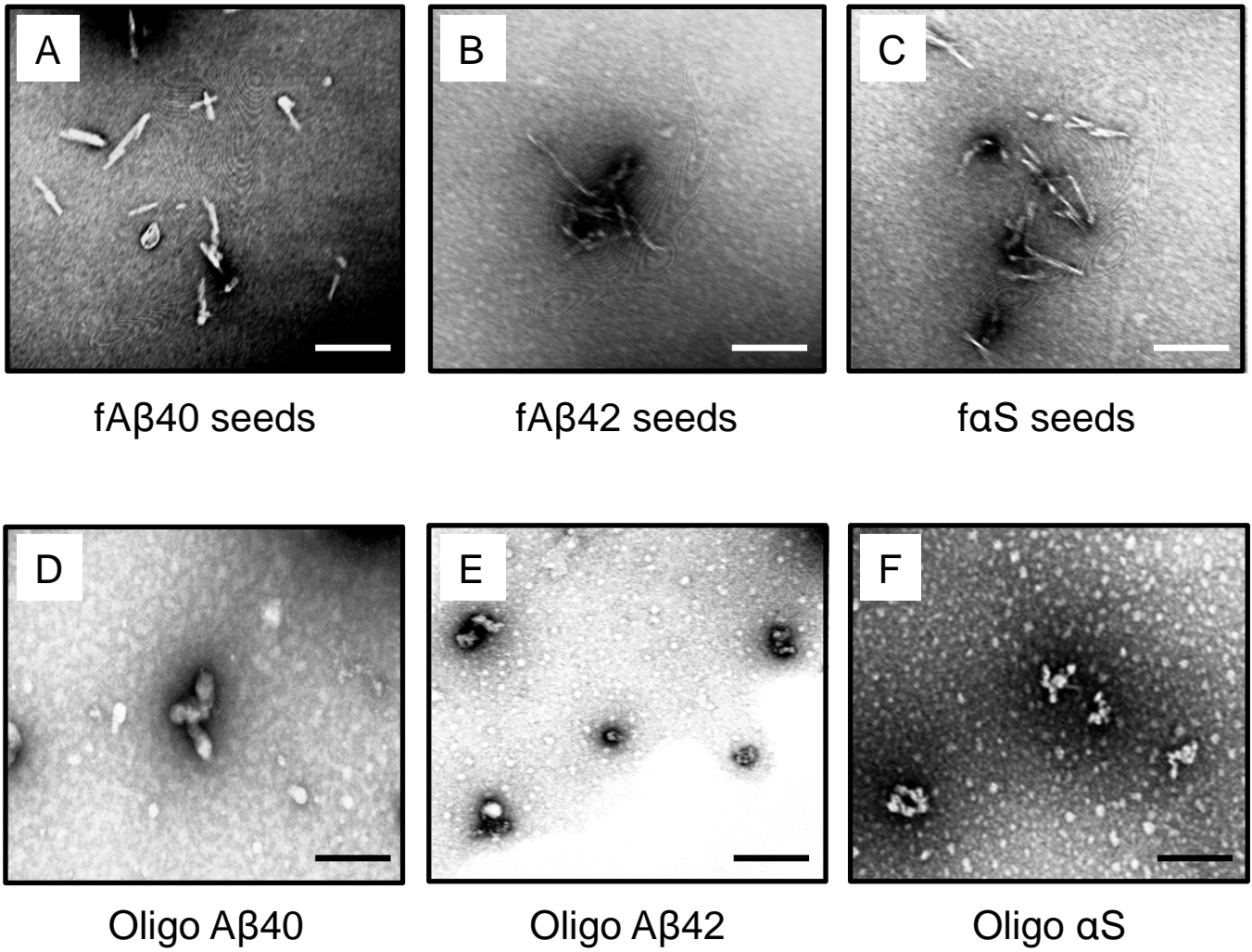
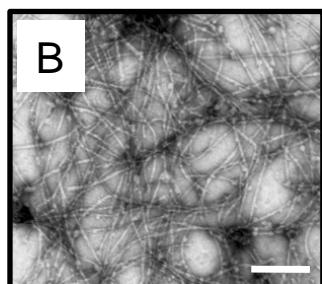
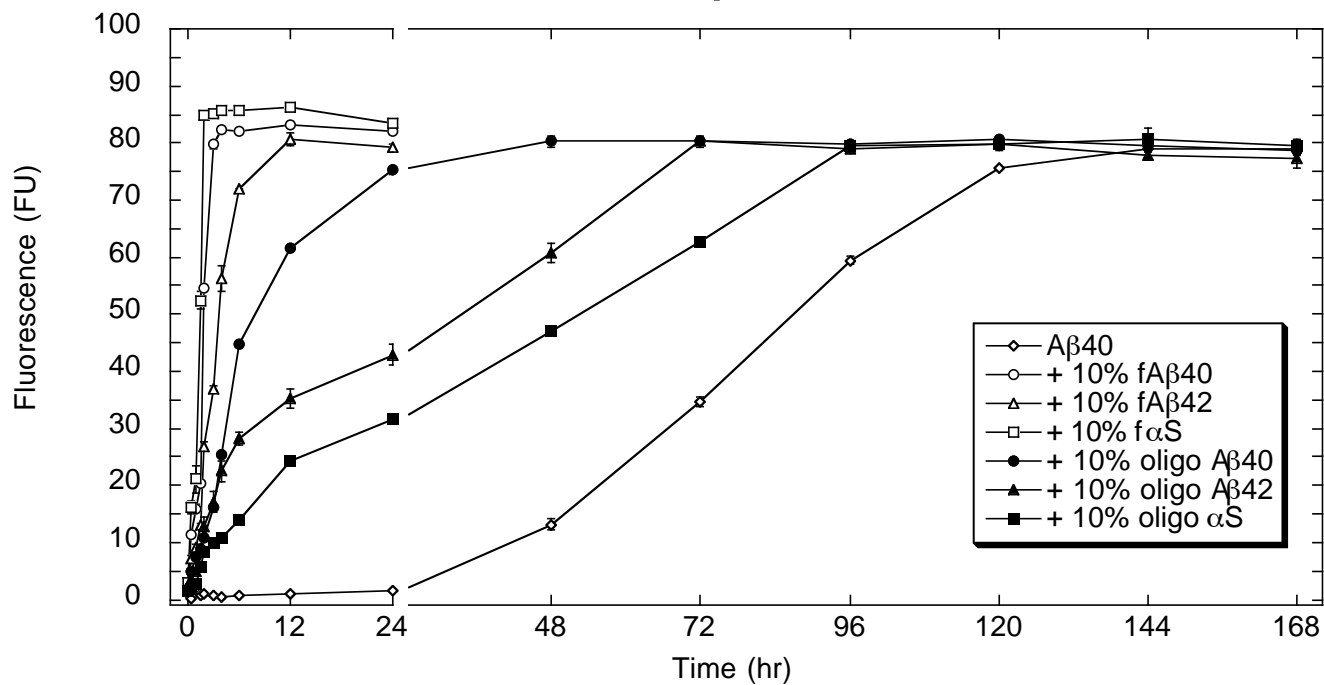


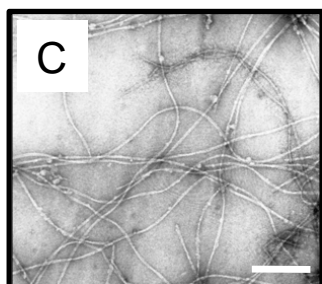
Fig. 2.

A

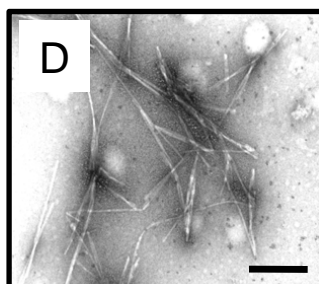
A $\beta$ 40



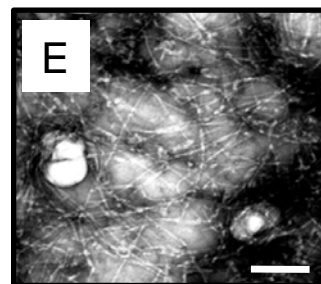
A $\beta$ 40



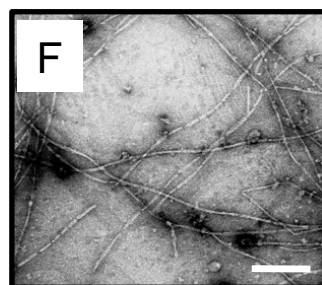
A $\beta$ 40 + fA $\beta$ 40



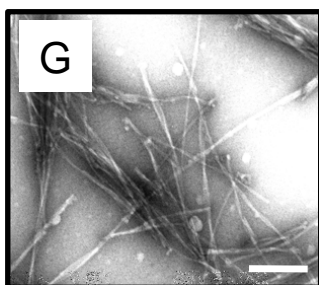
A $\beta$ 40 + fA $\beta$ 42



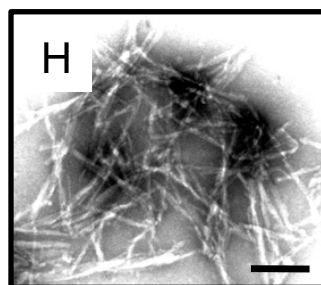
A $\beta$ 40 + f $\alpha$ S



A $\beta$ 40 + oligo A $\beta$ 40



A $\beta$ 40 + oligo A $\beta$ 42

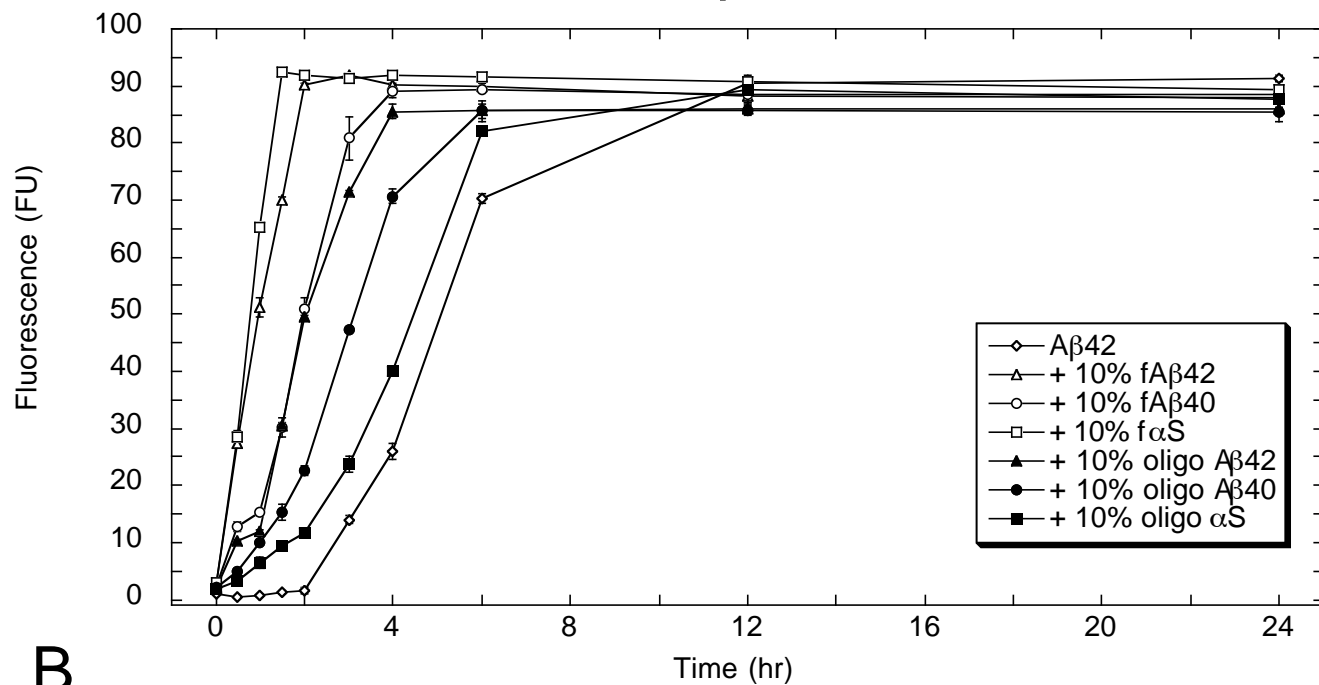


A $\beta$ 40 + oligo  $\alpha$ S

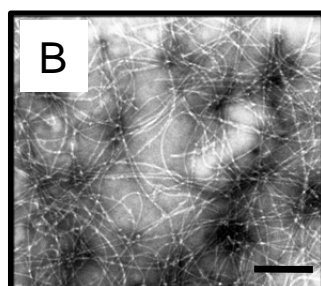
Fig. 3.

A

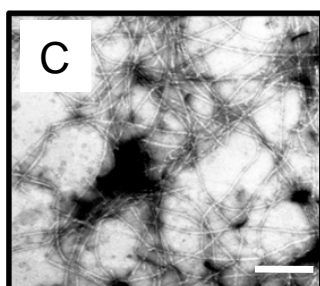
A $\beta$ 42



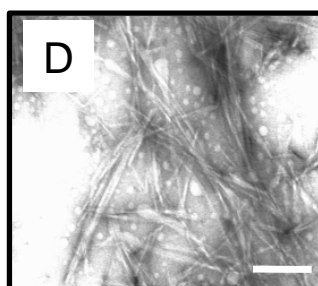
B



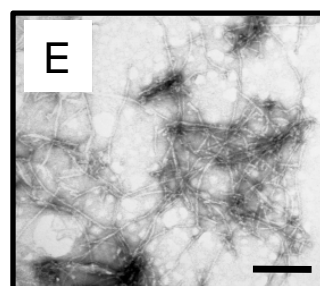
A $\beta$ 42



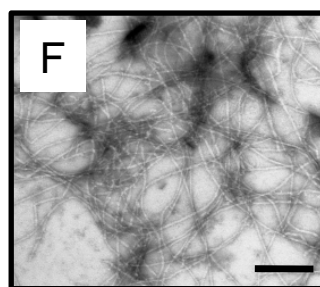
A $\beta$ 42 + fA $\beta$ 42



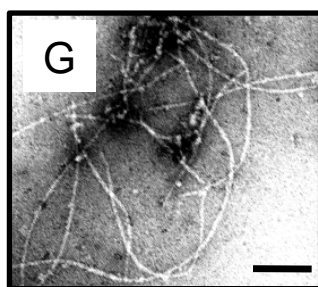
A $\beta$ 42 + fA $\beta$ 40



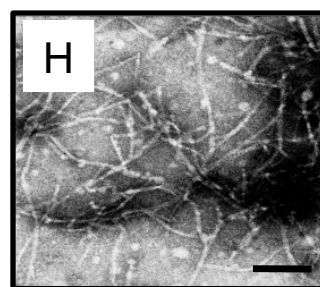
A $\beta$ 42 + f $\alpha$ S



A $\beta$ 42 + oligo A $\beta$ 42



A $\beta$ 42 + oligo A $\beta$ 40

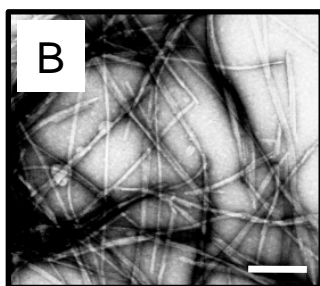
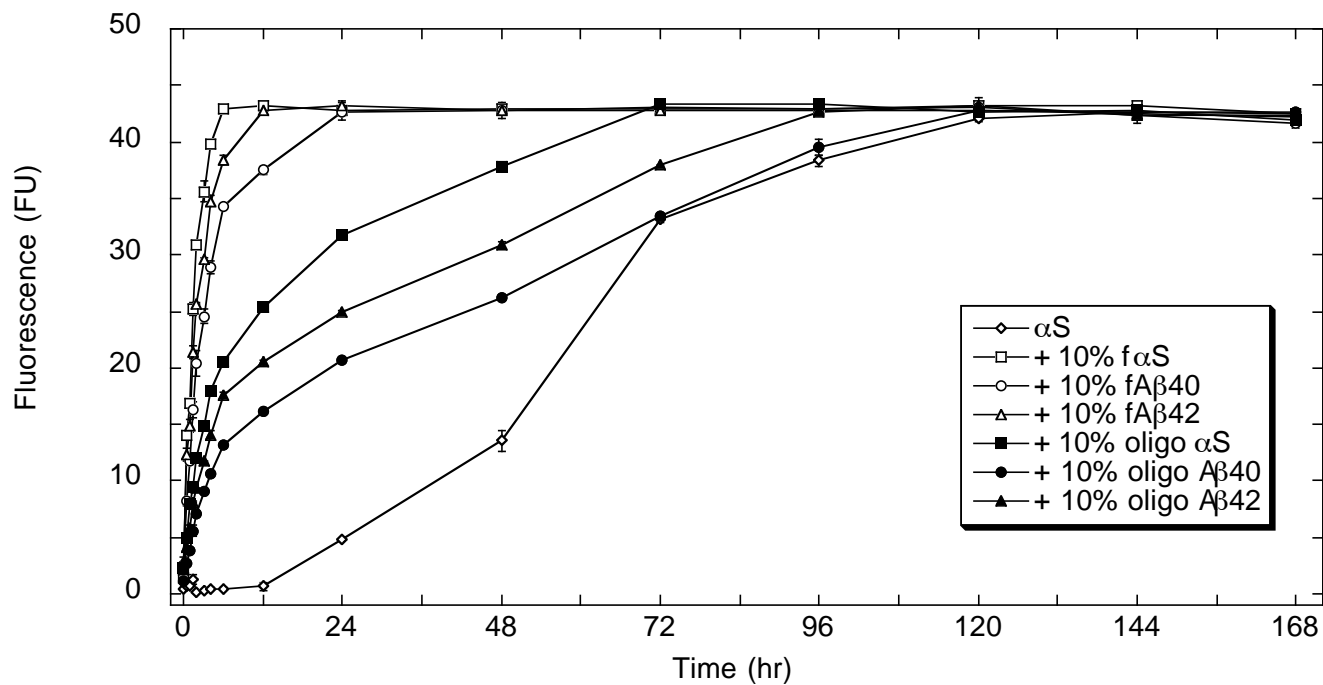


A $\beta$ 42 + oligo  $\alpha$ S

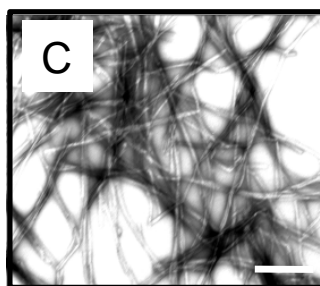
Fig. 4.

A

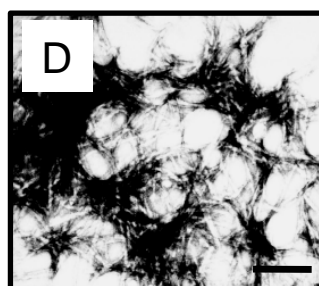
$\alpha$ S



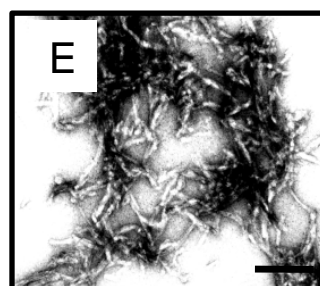
$\alpha$ S



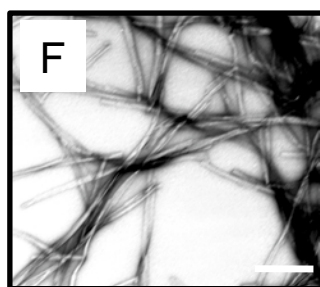
$\alpha$ S + f $\alpha$ S



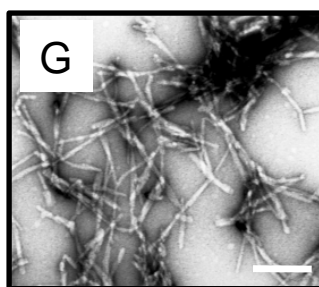
$\alpha$ S + fA $\beta$ 40



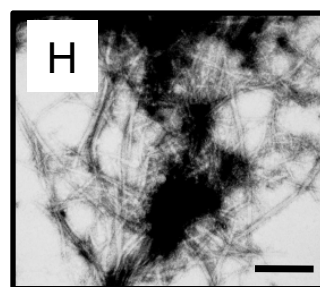
$\alpha$ S + fA $\beta$ 42



$\alpha$ S + oligo  $\alpha$ S



$\alpha$ S + oligo A $\beta$ 40



$\alpha$ S + oligo A $\beta$ 42